This article was downloaded by: [Institute Of Atmospheric Physics]
On: 09 December 2014, At: 15:32
Publisher: Taylor & Francis
Informa Ltd Registered in England and Wales Registered Number: 1072954 Registered office: Mortimer House, 37-41 Mortimer Street, London W1T 3JH, UK

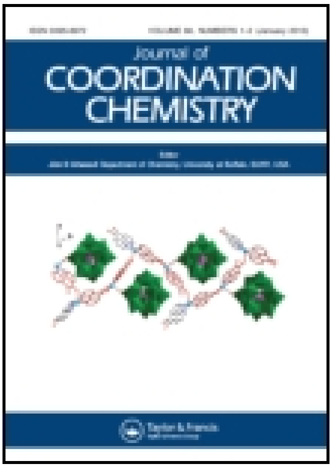

Click for updates

Journal of Coordination Chemistry

Publication details, including instructions for authors and subscription information:
http://www.tandfonline.com/loi/gcoo20

Syntheses and structural determination of binuclear nine-coordinate $(NH_4)_4[Sm^{III}_2(Httha)_2]\cdot 16H_2O$ and 2-D ladder-like binuclear nine-coordinate $(NH_4)_4[Sm^{III}_2(dtpa)_2]\cdot 10H_2O$

Congcong Ma[a], Ying Li[a], Jun Wang[a], Cui Qin[a], Deyong Kong[a], Jingqun Gao[a] & Qiong Wu[a]
[a] College of Chemistry, Liaoning University, Shenyang, PR China

Accepted author version posted online: 10 Feb 2014.Published online: 10 Mar 2014.

To cite this article: Congcong Ma, Ying Li, Jun Wang, Cui Qin, Deyong Kong, Jingqun Gao & Qiong Wu (2014) Syntheses and structural determination of binuclear nine-coordinate $(NH_4)_4[Sm^{III}_2(Httha)_2]\cdot 16H_2O$ and 2-D ladder-like binuclear nine-coordinate $(NH_4)_4[Sm^{III}_2(dtpa)_2]\cdot 10H_2O$, Journal of Coordination Chemistry, 67:4, 597-610, DOI: 10.1080/00958972.2014.892074

To link to this article: http://dx.doi.org/10.1080/00958972.2014.892074

PLEASE SCROLL DOWN FOR ARTICLE

Taylor & Francis makes every effort to ensure the accuracy of all the information (the “Content”) contained in the publications on our platform. However, Taylor & Francis, our agents, and our licensors make no representations or warranties whatsoever as to the accuracy, completeness, or suitability for any purpose of the Content. Any opinions and views expressed in this publication are the opinions and views of the authors, and are not the views of or endorsed by Taylor & Francis. The accuracy of the Content should not be relied upon and should be independently verified with primary sources of information. Taylor and Francis shall not be liable for any losses, actions, claims, proceedings, demands, costs, expenses, damages, and other liabilities whatsoever or howsoever caused arising directly or indirectly in connection with, in relation to or arising out of the use of the Content.

This article may be used for research, teaching, and private study purposes. Any substantial or systematic reproduction, redistribution, reselling, loan, sub-licensing,

Journal of Coordination Chemistry, 2014
Vol. 67, No. 4, 597–610, http://dx.doi.org/10.1080/00958972.2014.892074

Syntheses and structural determination of binuclear nine-coordinate $(NH_4)_4[Sm^{III}_2(Httha)_2]\cdot 16H_2O$ and 2-D ladder-like binuclear nine-coordinate $(NH_4)_4[Sm^{III}_2(dtpa)_2]\cdot 10H_2O$

CONGCONG MA, YING LI, JUN WANG*, CUI QIN, DEYONG KONG,
JINGQUN GAO and QIONG WU

College of Chemistry, Liaoning University, Shenyang, PR China

(*Received 18 October 2013; accepted 7 January 2014*)

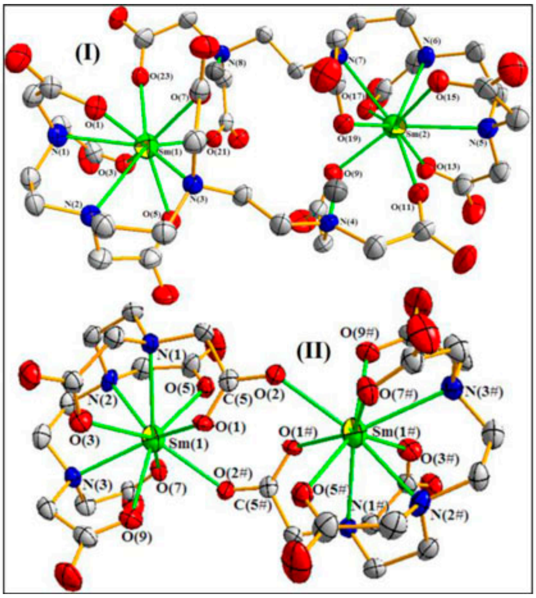

Two Sm^{III} coordination compounds, $(NH_4)_4[Sm^{III}_2(Httha)_2]\cdot 16H_2O$ (I) (H_6ttha = triethylenetetramine-*N,N,N′,N″,N‴,N‴*-hexaacetic acid) and $(NH_4)_4[Sm^{III}_2(dtpa)_2]\cdot 10H_2O$ (II) (H_5dtpa = diethylenetriamine-*N,N,N′,N″,N″*-pentaacetic acid), were synthesized. The complex (I) takes binuclear molecule structural nine-coordinate tricapped trigonal prismatic conformation. The complex (II) also takes binuclear molecule structural nine-coordinate tricapped trigonal prismatic conformation, but forms polymeric 2-D ladder-like layer structure through hydrogen bonds.

---

*Corresponding author. Email: wangjuncomplex890@126.com

Two rare-earth metal coordination compounds, $(NH_4)_4[Sm^{III}_2(Httha)_2]\cdot 16H_2O$ (**1**) (H_6ttha = triethylenetetramine-*N,N,N′,N″,N‴,N‴*-hexaacetic acid) and $(NH_4)_4[Sm^{III}_2(dtpa)_2]\cdot 10H_2O$ (**2**) (H_5dtpa = diethylenetriamine-*N,N,N′,N″,N″*-pentaacetic acid), have been synthesized through reflux and characterized by FT-IR spectroscopy, thermal analysis, and single-crystal X-ray diffraction techniques. Sm^{III} of $(NH_4)_4[Sm^{III}_2(Httha)_2]\cdot 16H_2O$ (**1**) is nine-coordinate, forming tricapped trigonal prismatic coordination with three amine nitrogens and six oxygens, in which four oxygens are from one ttha and two from the other ttha. $(NH_4)_4[Sm^{III}_2(Httha)_2]\cdot 16H_2O$ (**1**) crystallizes in the monoclinic crystal system with *P2(1)/c* space group. The crystal data are: $a = 13.9340(13)$ Å, $b = 22.890(3)$ Å, $c = 20.708(2)$ (14) Å, $\beta = 99.521(2)°$, and $V = 6513.7(13)$ $Å^3$. There are two $–NH^+–$ groups in the $[Sm^{III}_2(Httha)_2]^{4-}$. The polymeric $(NH_4)_4[Sm^{III}_2(dtpa)_2]\cdot 10H_2O$ (**2**) also is nine-coordinate with tricapped trigonal prismatic conformation and crystallizes in the triclinic crystal system with *P*–1 space group. The cell dimensions are: $a = 9.8240(8)$ Å, $b = 10.0329(9)$ Å, $c = 13.0941(11)$ Å, $\beta = 77.1640(10)°$, and $V = 1227.30(18)$ $Å^3$. In $(NH_4)_4[Sm^{III}_2(dtpa)_2]\cdot 10H_2O$, there are two types of ammonium cations, which connect $[Sm^{III}_2(dtpa)_2]^{4-}$ and lattice water through hydrogen bonds, leading to a 2-D ladder-like layer structure.

Keywords: Sm^{III}; Triethylenetetramine-*N,N,N′,N″,N‴,N‴*-hexaacetic acid (H_6ttha); Diethylenetriamine-*N,N,N′,N″,N″*-pentaacetic acid (H_5dtpa); Ammonia (NH_3); Hydrogen bond

1. Introduction

Rare-earth metal complexes attract a great deal of attention all through owing to their intriguing frameworks and potential applications [1, 2]. Particularly, they were often used for medical diagnostics, for example, as shift reagents for nuclear magnetic resonance spectroscopy [3–5], luminescent chemosensors [6, 7] and probes [8, 9]. For instance, Tb^{III} and Eu^{III} complexes, as fluorescence probes, have been used to diagnose some diseases [10, 11]. The $4f(^1G_4)–4f(^3H_6)$ electronic transition of Tm^{3+} provides a spectrally narrow blue light emission at 480 nm [12], which will benefit full-color flat display. In particular, the $^{153}Sm^{III}$ complexes as radioactive drugs expand treatment options for osteosarcoma, offering patients with bone cancer a treatment that specifically targets and kills tumor cells in the bone [13–16]. $^{153}Sm^{III}$-EDTMP (EDTMP = ethylenediamine-*N*,*N*,*N′*,*N′*-tetramethylenephosphonate) has been reported as a high-efficiency and long-lasting treatment of nasopharyngeal, breast carcinoma, lung cancer, and prostate carcinoma [17, 18]. ^{153}Sm(III) complexes with aminopolycarboxylic acid ligands are used as palliative agents for painful bone metastasis and follow the distribution of radionuclide *in vivo* [19–21]. Because Sm^{III} can yield stable complexes and construct various perfect coordinate structures with aminopolycarboxylic acid ligands, it should enter into the body as stable complexes having selectivity and affinity on the focus position and quickly be evacuated from the body after diagnosis or therapy [21, 22]. Thus, Sm^{III} complexes with aminopolycarboxylic acid ligands have wide applications in medicine. The major roles of Sm^{III} complexes in biology encourage us to further study the molecular structure and coordinate structure of Sm^{III} complexes with aminopolycarboxylic acid ligands.

A series of Sm^{III} complexes with aminopolycarboxylic acid ligands have been reported, $\{[Sm^{III}(Hpdta)(H_2O)]\cdot 2H_2O\}_n$ (H_4pdta = propylenediamine-*N,N,N′,N′*-tetraacetic acid) [23], $(enH_2)_{1.5}[Sm^{III}(ttha)]\cdot 4.5H_2O$ (H_6ttha = triethylenetetramine-*N,N,N′,N″,N‴,N‴*-hexaacetic acid) [24] and $Na_2[Sm^{III}(cydta)][Sm^{III}(cydta)(H_2O)_3]\cdot 11H_2O$ (H_4cydta = trans-1,2-cyclohexanediamine-*N,N,N′,N′*-tetraacetic acid) [25]. Sm^{III} complexes can adopt coordination number eight or nine, and the coordinate structure can take pseudo-monocapped square antiprismatic, pseudo-square antiprismatic, or tricapped trigonal prismatic geometry. However, there are few reports on the ammonium salts of Sm^{III} complexes. Our studies showed that the coordination numbers and coordinate structures of rare-earth metal complexes with aminopolycarboxylic acid ligands related to the shape of ligands and also the counter ion. We want to know how ammonium and ligand species affect coordination number, coordinate structure, space group, molecular structure, and crystal structure. Nitrogen is an integral part of DNA and proteins; through research on the binding between ammonium with rare-earth metal complex anions, we can compare interactions between these complexes with DNA or proteins. Therefore, binding between ammonium with rare-earth metal complex anions is significant for the exploration of their bioactivities and targets.

In order to extend our work, two aminopolycarboxylic acids, H_6ttha (= triethylenetetramine-*N,N,N′,N″,N″,N″*-hexaacetic acid) and H_5dtpa (= diethylenetriamine-*N,N,N′,N″,N″*-pentaacetic acid), were chosen as ligands and ammonium as counter ion, giving two samarium complexes with aminopolycarboxylic acid ligands, $(NH_4)_4[Sm^{III}_2(Httha)_2]\cdot 16H_2O$ (**1**) and $(NH_4)_4[Sm^{III}_2(dtpa)_2]\cdot 10H_2O$ (**2**), through direct heating. The molecular and crystal structures were characterized by FT-IR spectra, thermal analyses, and single-crystal X-ray diffraction.

2. Experimental setup

2.1. *Syntheses*

2.1.1. $(NH_4)_4[Sm^{III}_2(Httha)_2]\cdot 16H_2O$ (1). H_6ttha (= triethylenetetramine-*N,N,N′,N″,N‴,N‴*-hexaacetic acid) (A.R., Beijing SHLHT Science & Trade Co. Ltd, China) (2.4723 g, 5.0 mM) was added to 100 mL warm water and Sm_2O_3 powder (99.999%, Yuelong Rare Earth Co. Ltd, China) (0.8718 g, 2.5 mM) was added slowly to the above solution. After the mixture had been stirred and refluxed for 15.0 h, the solution became transparent and the pH was adjusted to 5.5 by dilute NH_3 aqueous solution. Finally, the solution was concentrated to 25 mL. A yellow crystal appeared after three weeks at room temperature.

2.1.2. $(NH_4)_4[Sm^{III}_2(dtpa)_2]\cdot 10H_2O$ (2). H_5dtpa (= diethylenetriamine-*N,N,N′,N″,N″*-pentaacetic acid) (A.R., Beijing SHLHT Science & Trade Co. Ltd, China) (1.9668 g, 5.0 mM) was added to 100 mL warm water and Sm_2O_3 powder (99.999%, Yuelong Rare Earth Co. Ltd, China) (0.8718 g, 2.5 mM) was added to the above solution slowly. The solution became transparent after the mixture had been stirred and refluxed for 13.0 h. Then, the pH was adjusted to 5.5 by dilute NH_3 aqueous solution. Finally, the solution was concentrated to 25 mL. A yellow crystal appeared after three weeks at room temperature.

2.2. *FT-IR spectroscopy*

The H_6ttha, H_5dtpa, **1** and **2** samples were skived and pressed to slices with KBr and their FT-IR spectra were determined by a Schimadza-IR 408 spectrophotometer. The obtained results are shown in Supplementary material (see online supplemental material at http://dx.doi.org/10.1080/00958972.2014.892074).

2.3. *Determination of TG-DTA*

Thermal analyses of **1** and **2** were conducted using a Mettler-Toledo 851° thermogravimetric analyzer in a flow of Ar (20 mL min^{-1}) from room temperature to 800 °C at a heating rate of 20 °C min^{-1}. The thermograms are shown in Supplementary material.

2.4. *X-ray structure determination*

The X-ray intensity data were collected on a Bruker SMART CCD type X-ray diffractometer system with graphite-monochromated Mo Kα radiation ($\lambda = 0.71073$ Å) at 298 K using φ-ω scan technique from $1.72° \leq \theta \leq 26.00°$. The structure was solved by direct methods. All nonhydrogen atoms were refined anisotropically by full-matrix least-squares method on F^2. All calculations were performed by SHELXTL-97 on PDP11/44 and Pentium MMX/166 computers. The crystal data and structure refinements are listed in table 1. Final atomic coordinates and equivalent isotropic displacement parameters for all nonhydrogen fractions are presented in Supplementary material. Selected bond distances and angles are listed in table 2. Some hydrogen bond distances (Å) and angles of **2** are listed in Supplementary material.

3. Results and discussion

3.1. *FT-IR spectra*

3.1.1. $(NH_4)_4[Sm^{III}_2(Httha)_2]\cdot16H_2O$ (1). The comparison of FT-IR spectra between H_6ttha and **1** (shown in Supplementary material) reveals that $\nu_{(C–N)}$ of **1** at 923 cm^{-1} blueshift by 24 cm^{-1} compared with that (899 cm^{-1}) of H_6ttha. This indicates that some nitrogens from ttha coordinate with Sm^{III}. The spectrum of free H_6ttha shows strong

Table 1. Crystal data and structure refinement for **1** and **2**.

Complex	1	2
Empirical formula	$C_{36}H_{98}N_{12}O_{40}Sm_2$	$C_{28}H_{72}N_{10}O_{30}Sm_2$
Formula weight	1639.96	1329.66
Temperature, K	298(2)	298(2)
Wavelength, Å	0.71073	0.71073
Crystal system	Monoclinic	Triclinic
Space group	*P2(1)/n*	*P–1*
Unit cell dimensions		
a, Å	13.9340(13)	9.8240(8)
b, Å	22.890(3)	10.0329(9)
c, Å	20.708(2)	13.0941(11)
β, deg	99.521(2)	77.1640(10)
Volume, Å^3	6513.7(13)	1227.30(18)
Z	4	1
ρ_{Calcd}, Mg/m^3	1.672	1.799
Absorption coefficient, mm^{-1}	1.892	2.472
F(000)	3368	674
Crystal size, mm	0.35 × 0.30 × 0.27	0.18 × 0.12 × 0.10
θ_{range} for data collection,°	2.42–25.02	2.60–25.02
Limiting indices	$-15 \leq h \leq 16$	$-11 \leq h \leq 11$
	$-27 \leq k \leq 20$	$-11 \leq k \leq 11$
	$-24 \leq l \leq 22$	$-15 \leq l \leq 9$
Reflections collected	32589	6206
Independent reflections	11482 [*R*(int) = 0.0546]	4242 [*R*(int) = 0.0319]
Completeness to θ_{max}, %	99.8	97.7
Max. and min. transmission	0.6291 and 0.5572	0.7901 and 0.6646
Goodness-of-fit on F^2	1.078	1.124
Final *R* indices [$I > 2\sigma(I)$]	$R1 = 0.0430$, $wR2 = 0.0958$	$R1 = 0.0453$, $wR2 = 0.0937$
R indices (all data)	$R1 = 0.0751$, $wR2 = 0.1189$	$R1 = 0.0586$, $wR2 = 0.1015$
Largest difference peak and hole, eÅ^{-3}	1.012 and −0.679	1.316 and −0.981
Absorption correction	Empirical	
Refinement method	Full-matrix least-squares on F^2	

Table 2. Selected bond distances (Å) and angles (deg) of **1** and **2**.

Bond	**d, Å**	**Bond**	**d, Å**	**Bond**	**d, Å**
1					
Sm(1)–O(1)	2.418(4)	Sm(1)–N(1)	2.662(5)	Sm(2)–O(15)	2.394(4)
Sm(1)–O(3)	2.411(5)	Sm(1)–N(2)	2.655(5)	Sm(2)–O(17)	2.405(5)
Sm(1)–O(5)	2.437(5)	Sm(1)–N(3)	2.746(5)	Sm(2)–O(19)	2.451(4)
Sm(1)–O(7)	2.467(4)	Sm(2)–O(9)	2.412(4)	Sm(2)–N(5)	2.696(5)
Sm(1)–O(21)	2.412(4)	Sm(2)–O(11)	2.379(5)	Sm(2)–N(6)	2.663(6)
Sm(1)–O(23)	2.388(5)	Sm(2)–O(13)	2.452(4)	Sm(2)–N(7)	2.724(5)
2					
Sm(1)–O(1)	2.402(4)	Sm(1)–O(5)	2.437(4)	Sm(1)–N(1)	2.729(5)
Sm(1)–O(2$^{\#1}$)	2.460(4)	Sm(1)–O(7)	2.421(4)	Sm(1)–N(2)	2.611(5)
Sm(1)–O(3)	2.428(4)	Sm(1)–O(9)	2.422(4)	Sm(1)–N(3)	2.644(5)
Angle	**ω, deg**	**Angle**	**ω, deg**	**Angle**	**ω, deg**
1					
O(1)–Sm(1)–O(3)	128.59(15)	O(7)–Sm(1)–N(2)	121.87(15)	O(11)–Sm(2)–N(5)	73.83(16)
O(1)–Sm(1)–O(5)	133.22(15)	O(7)–Sm(1)–N(3)	61.30(15)	O(11)–Sm(2)–N(6)	141.64(16)
O(1)–Sm(1)–O(7)	71.36(14)	O(21)–Sm(1)–O(23)	78.53(14)	O(11)–Sm(2)–N(7)	135.81(16)
O(1)–Sm(1)–O(21)	140.19(15)	O(21)–Sm(1)–N(1)	138.77(16)	O(13)–Sm(2)–O(15)	126.27(15)
O(1)–Sm(1)–O(23)	81.84(15)	O(21)–Sm(1)–N(2)	139.07(15)	O(13)–Sm(2)–O(17)	71.06(16)
O(1)–Sm(1)–N(1)	64.82(15)	O(21)–Sm(1)–N(3)	91.39(15)	O(13)–Sm(2)–O(19)	146.48(17)
O(1)–Sm(1)–N(2)	71.95(16)	O(23)–Sm(1)–N(1)	74.18(16)	O(13)–Sm(2)–N(5)	62.56(16)
O(1)–Sm(1)–N(3)	78.05(15)	O(23)–Sm(1)–N(2)	141.08(15)	O(13)–Sm(2)–N(6)	91.16(18)
O(3)–Sm(1)–O(5)	72.62(16)	O(23)–Sm(1)–N(3)	134.10(15)	O(13)–Sm(2)–N(7)	143.43(16)
O(3)–Sm(1)–O(7)	144.13(15)	N(1)–Sm(1)–N(2)	68.85(17)	O(15)–Sm(2)–O(17)	134.66(16)
O(3)–Sm(1)–O(21)	81.50(16)	N(1)–Sm(1)–N(3)	129.72(16)	O(15)–Sm(2)–O(19)	70.33(15)
O(3)–Sm(1)–O(23)	81.84(15)	N(2)–Sm(1)–N(3)	68.12(16)	O(15)–Sm(2)–N(5)	63.82(15)
O(3)–Sm(1)–N(1)	64.00(16)	O(11)–Sm(2)–O(9)	77.08(16)	O(15)–Sm(2)–N(6)	72.69(17)
O(3)–Sm(1)–N(2)	93.91(17)	O(9)–Sm(2)–O(13)	84.71(16)	O(15)–Sm(2)–N(7)	77.86(15)
O(3)–Sm(1)–N(3)	142.89(16)	O(9)–Sm(2)–O(15)	139.38(16)	O(17)–Sm(2)–O(19)	120.70(15)
O(5)–Sm(1)–O(7)	118.06(14)	O(9)–Sm(2)–O(17)	75.62(16)	O(17)–Sm(2)–N(5)	111.55(17)
O(5)–Sm(1)–O(21)	75.21(15)	O(9)–Sm(2)–O(19)	70.15(15)	O(17)–Sm(2)–N(6)	64.82(17)
O(5)–Sm(1)–O(23)	144.50(15)	O(9)–Sm(2)–N(5)	139.55(16)	O(17)–Sm(2)–N(7)	72.75(15)
O(5)–Sm(1)–N(1)	112.04(17)	O(9)–Sm(2)–N(6)	139.27(16)	O(19)–Sm(2)–N(5)	126.05(15)
O(5)–Sm(1)–N(2)	64.74(16)	O(9)–Sm(2)–N(7)	91.40(15)	O(19)–Sm(2)–N(6)	122.36(16)
O(5)–Sm(1)–N(3)	70.35(15)	O(11)–Sm(2)–O(13)	78.63(17)	O(19)–Sm(2)–N(7)	61.55(15)
O(7)–Sm(1)–O(21)	69.95(14)	O(11)–Sm(2)–O(15)	83.80(16)	N(5)–Sm(2)–N(6)	68.72(17)
O(7)–Sm(1)–O(23)	73.28(14)	O(11)–Sm(2)–O(17)	140.59(17)	N(5)–Sm(2)–N(7)	129.02(16)
O(7)–Sm(1)–N(1)	128.05(16)	O(11)–Sm(2)–O(19)	74.49(15)	N(6)–Sm(2)–N(7)	68.61(16)
2					
O(1)–Sm(1)–O(2$^{\#1}$)	72.45(14)	O(2$^{\#1}$)–Sm(1)–N(1)	124.89(14)	O(5)–Sm(1)–N(2)	66.75(15)
O(1)–Sm(1)–O(3)	81.21(14)	O(2$^{\#1}$)–Sm(1)–N(2)	137.89(15)	O(5)–Sm(1)–N(3)	127.13(15)
O(1)–Sm(1)–O(5)	89.79(14)	O(2$^{\#1}$)–Sm(1)–N(3)	115.69(16)	O(7)–Sm(1)–O(9)	93.78(16)
O(1)–Sm(1)–O(7)	142.71(14)	O(3)–Sm(1)–O(5)	131.88(16)	O(7)–Sm(1)–N(1)	136.63(15)
O(1)–Sm(1)–O(9)	85.30(15)	O(3)–Sm(1)–O(7)	134.22(15)	O(7)–Sm(1)–N(2)	74.24(16)
O(1)–Sm(1)–N(1)	61.90(14)	O(3)–Sm(1)–O(9)	73.51(16)	O(7)–Sm(1)–N(3)	65.71(15)
O(1)–Sm(1)–N(2)	130.41(16)	O(3)–Sm(1)–N(1)	63.60(15)	O(9)–Sm(1)–N(1)	128.46(15)
O(1)–Sm(1)–N(3)	142.44(14)	O(3)–Sm(1)–N(2)	83.76(15)	O(9)–Sm(1)–N(2)	134.15(16)
O(2$^{\#1}$)–Sm(1)–O(3)	138.25(15)	O(3)–Sm(1)–N(3)	69.17(16)	O(9)–Sm(1)–N(3)	64.88(15)
O(2$^{\#1}$)–Sm(1)–O(5)	80.64(14)	O(5)–Sm(1)–O(7)	74.42(15)	N(1)–Sm(1)–N(2)	69.05(16)
O(2$^{\#1}$)–Sm(1)–O(7)	71.76(14)	O(5)–Sm(1)–O(9)	153.03(15)	N(1)–Sm(1)–N(3)	119.25(16)
O(2$^{\#1}$)–Sm(1)–O(9)	72.59(15)	O(5)–Sm(1)–N(1)	70.47(15)	N(2)–Sm(1)–N(3)	69.96(17)

Symmetry code: #1: −x + 1, −y + 1, −z + 1

absorptions at 1736 cm^{-1} originating from $\nu_{(C=O)}$, which disappears completely in the FT-IR spectrum of **1**. In addition, **1** gives the characteristic absorption of carboxyl at 1608 cm^{-1} for the asymmetric stretch and at 1400 cm^{-1} for the symmetric stretch, a blueshift (138 cm^{-1}) compared with 1470 cm^{-1} of H$_6$ttha and a redshift 14 cm^{-1} compared with that

(1414 cm^{-1}) of H_6ttha, indicating that oxygens of carboxyl are also coordinated. There is a broad absorption at 3428 cm^{-1} for **1**. It could be reasonably attributed to the stretching vibration of O–H.

3.1.2. $(NH_4)_4[Sm^{III}_2(dtpa)_2]\cdot 10H_2O$ (2). Similarly, as shown in Supplementary material, $\nu_{(C–N)}$ of **2** at 932 cm^{-1} displays a redshift (29 cm^{-1}) compared with that (961 cm^{-1}) of H_5dtpa, indicating that the amine nitrogens of H_5dtpa are coordinated to Sm^{III}. The characteristic absorption of carboxyl at 1597 cm^{-1} for asymmetric stretch and at 1403 cm^{-1} for symmetric stretch indicate that carboxyl groups are coordinated to Sm^{III}. Disappearance of strong absorption at 1734 cm^{-1} reveals that all carboxylic groups are completely deprotonated, consistent with results of X-ray diffraction analyses. A strong and broad absorption at 3425 cm^{-1} shows the existence of O–H in **2**.

3.2. *Thermal analyses*

3.2.1. $(NH_4)_4[Sm^{III}_2(Httha)_2]\cdot 16H_2O$ (1). The TG curve of **1** shows a four-stage decomposition (Supplementary material). The first weight loss is 8.0% from room temperature to 105 °C, which corresponds to the expulsion of ammonia. The second weight loss of 17.5% from 105 to 300 °C corresponds to the expulsion of lattice water. The third weight loss is attributed to the decomposition of organic ligand starting from 300 to 425 °C; the weight loss ratio is 28.97%. The last stage from 425 to 800 °C (weight loss of 14.4%) corresponds to the decomposition of carboxylate. The final residue is mainly Sm_2O_3 with total weight loss ratio of 68.87%.

3.2.2. $(NH_4)_4[Sm^{III}_2(dtpa)_2]\cdot 10H_2O$ (2). The thermal decomposition process of **2** is similar to that of **1** with three-stage decomposition (Supplementary material). The first decomposition happens from 25 to 100 °C with weight loss of 5.90%, which corresponds to the release of ammonia. The second weight loss (13.71%) from 100 to 271 °C corresponds to the expulsion of 10 lattice waters. Then, the sample decomposes gradually and the decomposition is completed at 800 °C. The corresponding weight loss is 51.84%, and the corresponding product is Sm_2O_3. The total weight loss ratio is 71.45%.

3.3. *Molecular and crystal structures*

3.3.1. $(NH_4)_4[Sm^{III}_2(Httha)_2]\cdot 16H_2O$ (1). $(NH_4)_4[Sm^{III}_2(Httha)_2]\cdot 16H_2O$ has a binuclear molecular structure (figure 1). In $[Sm^{III}_2(Httha)_2]^{4-}$, all carboxylic groups in the two H_6ttha are coordinated to two Sm^{III} ions, similar to $K_4[Eu^{III}_2(Httha)_2]\cdot 13.5H_2O$ [26], $K_4[Tb^{III}_2(Httha)_2]\cdot 14H_2O$ [26] and $K_4[Sm^{III}_2(Httha)_2]\cdot 14H_2O$ [27] reported previously. The Sm^{III} is coordinated with three amine nitrogens and four oxygens from one ttha and two oxygens from the other ttha. Due to the relatively high acidity of aqueous solution, when **1** was synthesized, two protons do not dissociate from the amine nitrogens of ttha and formed $\equiv NH^+$ so that the two protonated nitrogens (N(4) and N(8)) in ttha do not coordinate with Sm^{III}.

Differing from $K_4[Eu^{III}_2(Httha)_2]\cdot 13.5H_2O$ and $K_4[Sm^{III}_2(Httha)_2]\cdot 14H_2O$, whose coordinate geometries around Eu^{III} or Sm^{III} are nine-coordinate pseudo-monocapped square antiprismatic (MC-SAP) conformation, the coordinate geometry around Sm^{III} in

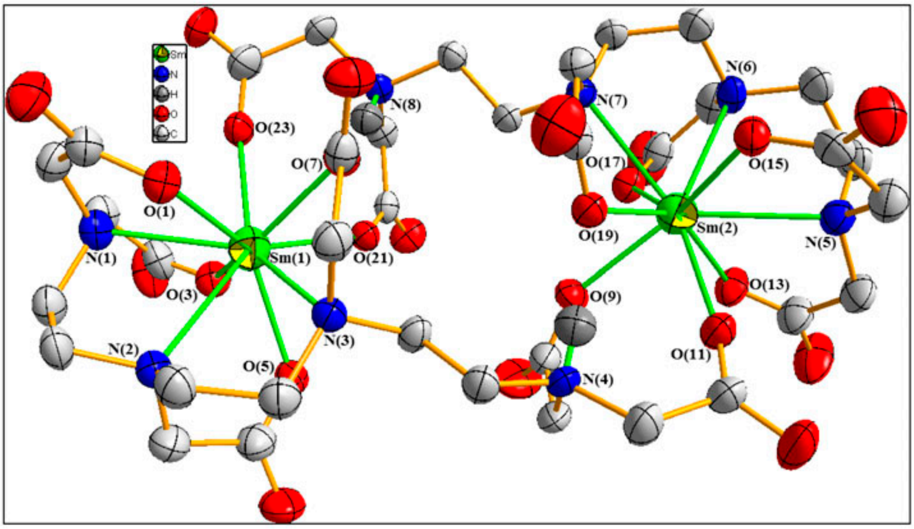

Figure 1. Molecular structure of **1**.

$[Sm^{III}_2(Httha)_2]^{4-}$ can be considered as nine-coordinate pseudo-tricapped trigonal prismatic (TC-TP) conformation (figure 2). Around Sm(1), O(1), N(2), and N(3) and the set of O(3), O(21), and O(23) form two approximately parallel trigonal planes, forming a trigonal prism. Three capped atoms, O(5) O(7), and N(1), lie above the planes formed by O(3), O(21), N(2), and N(3); O(1), O(21), O(23), and N(3); and O(1), O(3), O(23), and N(2), respectively. The total angle of ⟨(N(1)Sm(1)O(5)), ⟨(N(1)Sm(1)O(7)), and ⟨(O(5)Sm(1)O(7)) is 358.15°, close to 360°, indicating that Sm(1), O(5), O(7), and N(1) are in the same plane. Around Sm(2), the set O(15), N(6), and N(7) and O(9), O(11), and O(13) form two approximate parallel trigonal planes, forming a trigonal prism, also. Three capped atoms, O(17),

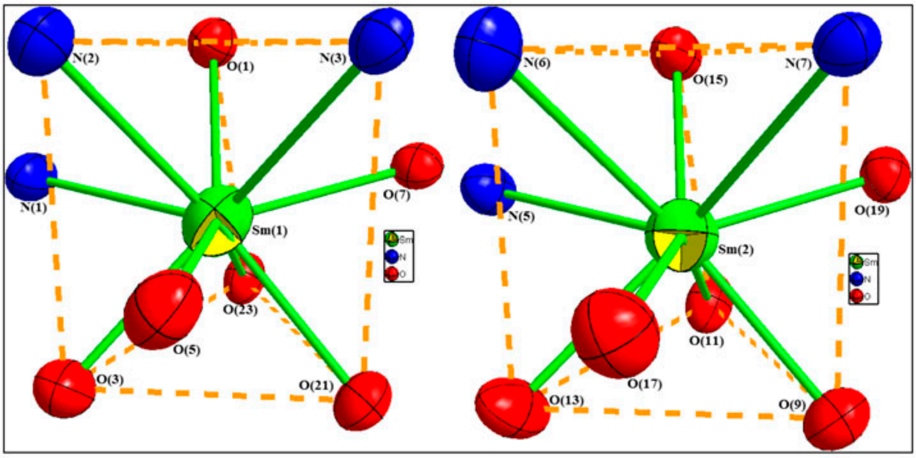

Figure 2. Coordination polyhedron around Sm^{III} in **1**.

O(19), and N(5), lie above the planes formed by O(9), O(13), N(6), and N(7); O(9), O(11), O(15), and N(7); and O(11), O(13), O(15), and N(6), respectively. The total angle of ⟨(N(1)Sm(1)O(5)), ⟨(N(1)Sm(1)O(7)), and ⟨(O(5)Sm(1)O(7)) is 358.31°, close to 360°, indicating that Sm(2), O(17), O(19), and N(5) are in the same plane.

For Sm(1), because of the repulsion between the capped [O(5), O(7), and N(1)] and the planes [formed by O(3), O(21), N(2), and N(3); O(1), O(21), O(23), and N(3); and O(1), O(3), O(23), and N(2)], $\mathrm{Sm(1)N_3O_6}$ is not a standard tricapped trigonal prismatic conformation. To the O(3)O(21)N(2)N(3) square plane, the value of trigonal dihedral angle is 2.66° between Δ(N(2)O(3)O(21)) and Δ(N(2)N(3)O(21)) and 2.74° between Δ(N(2)N(3)O(3)) and Δ(O(3)O(21)N(3)). To the O(1)O(21)O(23)N(3) square plane, the trigonal dihedral angle between Δ(O(21)N(3)O(23)) and Δ(N(3)O(23)O(1)) is 8.65° and between Δ(N(3)O(1)O(21)) and Δ(O(1)O(21)O(23)) is 8.40°. The trigonal dihedral angle between Δ(N(2)O(1)O(3)) and Δ(O(1)O(3)O(23)) is 11.97° and between Δ(O(1)N(2)O(23)) and Δ(N(2)O(23)O(3)) is 13.19°. The values of the trigonal dihedral angle tend to 0°, showing four atoms almost in the same plane. That is, these data predict that four atoms of every side of the triangular prism are almost located in the same plane. According to these calculated data, the conformation of $\mathrm{Sm(1)N_3O_6}$ in $[\mathrm{Sm^{III}}_2\mathrm{(Httha)_2}]^{4-}$ is a TC-TP conformation but distorts to a small extent. Similarly, for Sm(2), the $\mathrm{Sm(2)N_3O_6}$ is not standard tricapped trigonal prismatic conformation. To the O(9)O(13)N(6)N(7) square plane, the value of trigonal dihedral angle is 3.57° between Δ(N(7)N(6)O(9)) and Δ(N(6)O(9)O(13)) and 3.69° between Δ(N(6)N(7)O(13)) and Δ(N(7)O(13)O(9)). To the O(9)O(11)O(15)N(7) square plane, the trigonal dihedral angle between Δ(N(7)O(15)O(9)) and Δ(O(15)O(9)O(11)) is 5.99° and between Δ(O(15) N(7)O(11)) and Δ(N(7)O(11)O(9)) is 6.22°. To the O(11)O(13)O(15)N(6)) square plane, the trigonal dihedral angle between Δ(O(15)N(6)O(11)) and Δ(N(6)O(11)O(13)) is 15.25° and between Δ(N(6)O(15)O(13)) and ΔO(15)O(13)O(11)) is 13.79°. These values show four atoms of dihedral angle are in the same plane. According to these calculated data, the conformation of $\mathrm{Sm(2)N_3O_6}$ in $[\mathrm{Sm^{III}}_2\mathrm{(Httha)_2}]^{4-}$ keeps a TC-TP conformation. Therefore, $\mathrm{Sm(1)N_3O_6}$ and $\mathrm{Sm(2)N_3O_6}$ in $[\mathrm{Sm^{III}}_2\mathrm{(Httha)_2}]^{4-}$ adopt TC-TP conformation.

As shown in table 2, for Sm(1), the Sm(1)–O bond distances are 2.388(5) Å (Sm(1)–O(23)) to 2.467(4) Å (Sm(1)–O(7)), and the average value is 2.422(6) Å. The Sm(1)–N bond lengths are 2.655(5) Å (Sm(1)–N(2)) and 2.746(5) Å (Sm(1)–N(3)) with average of 2.688(2) Å. The O–Sm(1)–O bond angles are 71.36(14)° (⟨O(1)–Sm(1)–O(7)) to 144.50(15) (⟨O(5)–Sm(1)–O(23)), O–Sm(1)–N bond angles vary from 61.30(15)° (⟨O(7)–Sm(1)–N(3)) to 141.08(15)° (⟨O(23)–Sm(1)–N(2)), and the ⟨N–Sm(1)–N bond angles change from 68.12(16)° (⟨N(2)–Sm(1)–N(3)) to 129.72(16)° (⟨N(1)–Sm(1)–N(3)). For Sm(2), the Sm(2)–O bond distances are 2.379(5) Å (Sm(2)–O(11)) to 2.452(4) Å (Sm(2)–O(13)), and the average is 2.415(9) Å. The Sm(2)–N bond lengths are 2.663(6) Å (Sm(2)–N(6)) and 2.724(5) Å (Sm(2)–N(7)) with average of 2.694(9) Å. The O–Sm(2)–O bond angles are 70.15(15)° (⟨O(9)–Sm(2)–O(19)) to 146.48(17) (⟨O(13)–Sm(2)–O(19)), O–Sm(2)–N bond angles vary from 61.55(15)° (⟨O(19)–Sm(2)–N(7)) to 141.64(16)° (⟨O(11)–Sm(2)–N(6)), and the ⟨N–Sm(2)–N bond angles change from 68.61(16)° (⟨N(6)–Sm(2)–N(7)) to 129.02(16)° (⟨N(5)–Sm(2)–N(7)). Thus, the coordination polyhedron around Sm(1) and Sm(2) of **1** are similar, although there are some differences in bond lengths and angles.

As shown in figure 3, there are four $\mathrm{(NH_4)_4[Sm^{III}}_2\mathrm{(Httha)_2]\cdot 16H_2O}$ molecules in a unit cell, connected with lattice water and protonated ammonium ($\mathrm{NH_4}^+$) through hydrogen bonds, and then crystallize in a monoclinic system with *P2(1)/n* space group.

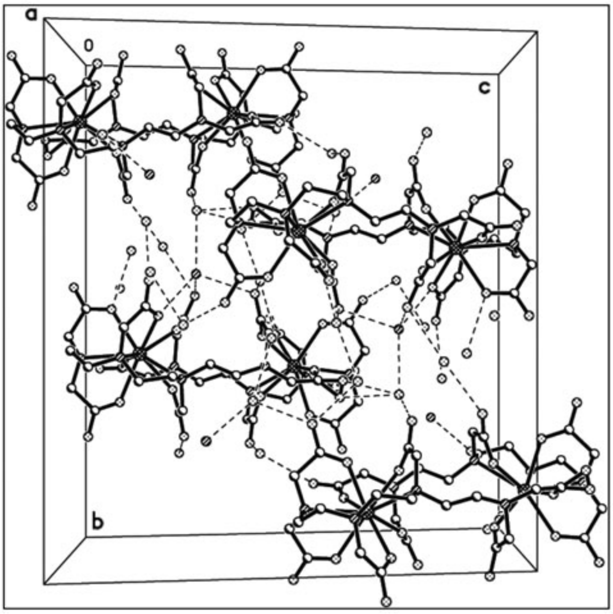

Figure 3. Arrangement of **1** in unit cell (dashed lines represent intermolecular hydrogen bonds).

3.3.2. $(NH_4)_4[Sm^{III}_2(dtpa)_2]\cdot 10H_2O$ (2). In this crystal structure, Sm^{III} forms a 1 : 1 complex with H_5dtpa. Although **2** is also binuclear nine-coordinate, its molecular and crystal structures are different from **1** because dtpa replaces ttha. Some similar findings were previously reported, $(NH_4)_4[Tb_2^{III}(dtpa)_2]\cdot 9H_2O$ [28] and $(NH_4)_4[Dy_2^{III}(dtpa)_2]\cdot 4H_2O$ [29]. Because NH_4^+ can form hydrogen bonds with complex anion and lattice water, shortening the distance of Sm(1) and Sm(1#), each dtpa contributes a carboxylic oxygen to coordinate to the adjacent Sm^{III} forming binuclear $[Sm^{III}_2(dtpa)_2]^{4-}$. Therefore, **2**, $(NH_4)_4[Tb_2^{III}(dtpa)_2]\cdot 9H_2O$ [28] and $(NH_4)_4[Dy_2^{III}(dtpa)_2]\cdot 4H_2O$ [29] all adopt binuclear structures, different from $K_2[Dy(dtpa)(H_2O)]\cdot 6H_2O$ [30] and $Na_4[Dy^{III}(dtpa)(H_2O)]_2\cdot 16H_2O$ [31], where K^+ and Na^+ combine with complex anions through an ionic bond, which cannot shorten the distance between complex anion units, resulting in mononuclear structures of these two complexes.

The molecular structure of **2** is shown in figure 4. Sm^{III} is nine-coordinate with three nitrogens and five carboxylic oxygens, which come from the same dtpa, and another oxygen from another dtpa. For $[Sm^{III}_2(dtpa)_2]^{4-}$, Sm(1) and Sm(1#) are centrosymmetric, and the symmetric center is located at the point of intersection of the two diagonals of the parallelogram formed by Sm(1), O(2), Sm(1#), and O(2#) (symmetry code: 1#: $-x+1$, $-y+1$, $-z+1$). As an octadentate ligand, dtpa is not able to supply enough donors to fill the coordination positions of Sm^{III}. Each dtpa coordinates to one Sm^{III} using its five carboxylic oxygens and three amine nitrogens. The ninth coordinated O(2#) is provided by another coordinated carboxylic group of dtpa. Therefore, O(2) and its symmetrically equivalent O (2#) play an important role in connecting Sm(1) and Sm(1#). In fact, the O(1)–C(5)–O(2) and O(1#)–C(5#)–O(2#) carboxylates connect Sm(1) and Sm(1#). Seven five-membered rings are formed in Sm(1) and Sm(1#) with the atoms of each ring being almost coplanar.

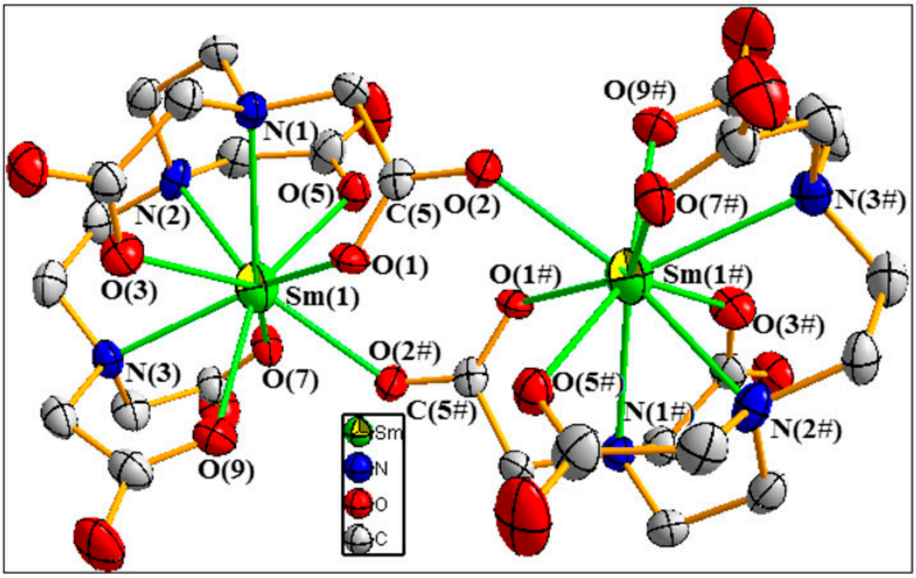

Figure 4. Molecular structure of **2**.

As seen from figure 5, the coordination polyhedron of $[\mathrm{Sm^{III}}_2(\mathrm{dtpa})_2]^{4-}$ is nine-coordinate pseudo-TC-TP. The upper triangle is formed by O(1), O(3), and O(9), while the nether triangle plane is formed by two carboxyl (O(5) and O(7)) and one amine nitrogen (N(2)). The first square plane is formed by three carboxyl (O(1), O(3), and O(5)) and one amine N(2).

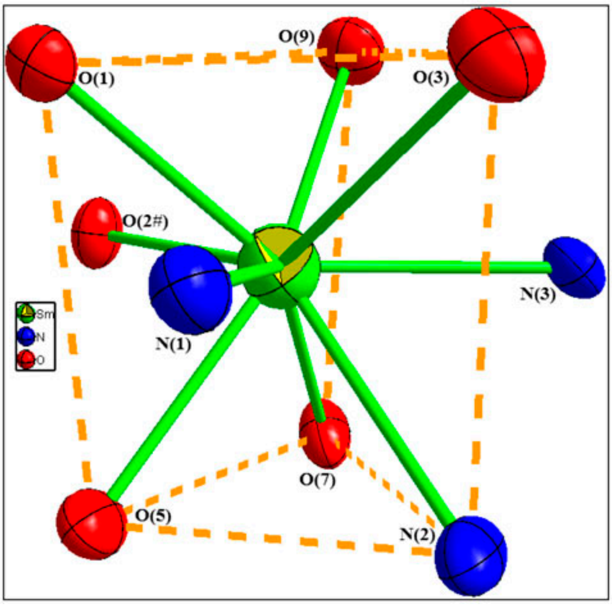

Figure 5. Coordination polyhedron around $\mathrm{Sm^{III}}$ in **2**.

The second square plane is formed by O(3), O(9), and O(7) and one amine N(2). And the third one is formed by four carboxyl (O(1), O(5), O(7), and O(9)). For these three square planes, the capping positions are occupied by two N(1) and N(3) and one carboxyl (O($2^{\#}$)), respectively.

As shown in table 2, because the O($2^{\#}$) comes from a bridging carboxylic group, the Sm (1)–O($2^{\#}$) bond distance (2.460(4) Å) is the longest of the Sm–O bonds. The Sm(1)–O bond distances in **2** are from 2.402(4) Å (Sm(1)–O(1)) to 2.460(4) Å (Sm(1)–O($2^{\#}$)), with average of 2.428(7) Å. The Sm(1)–N bond distances vary from 2.611(5) Å (Sm(1)–N(2)) to 2.729(5) Å (Sm(1)–N(1)), with average of 2.661(8) Å, longer than the Sm(1)–O bond distances, suggesting that O coordinates to $\mathrm{Sm^{III}}$ much stronger than N. The O–Sm(1)–O bond angles vary from 71.76(14)° (⟨(O($2^{\#}$)–Sm(1)–O(7)) to 153.03(15)° (⟨O(5)–Sm(1)–O(9)). The O–Sm(1)–N bond angles vary from 61.90(14)° (⟨O(1)–Sm(1)–N(1)) to 142.44(14)° (⟨O(1)–Sm(1)–N(3)), and the ⟨N–Sm(1)–N bond angles change from 69.05(16)° (N(1)–Sm (1)–N(2)) to 119.25(16)° (N(1)–Sm(1)–N(3)). The smallest and largest bond angles are 61.90(14)° (⟨O(1)–Sm(1)–N(1)) and 153.03(15)° (⟨O(5)–Sm(1)–O(9)), respectively.

In $\mathrm{Sm(1)N_3O_6}$ (figure 5), due to the repulsion between the capped atoms and the planes, the coordination polyhedron is not standard tricapped trigonal prismatic conformation. The values of the trigonal dihedral angle tend to 0°, indicating four atoms of the dihedral angle are almost in the same plane; these data predict that four atoms of every side of the triangular prism are almost located in the same plane. The conformation of $\mathrm{Sm(1)N_3O_6}$ in $[\mathrm{Sm^{III}}_2(\mathrm{dtpa})_2]^{4-}$ is a slightly distorted TC-TP.

As shown in figure 6, there is only one $(\mathrm{NH_4})_4[\mathrm{Sm^{III}}_2(\mathrm{dtpa})_2]\cdot 10\mathrm{H_2O}$ (**2**) in a unit cell. The complex molecule connects with lattice waters and ammonium ($\mathrm{NH_4^+}$) through hydrogen bonds, and then crystallize in triclinic crystal system with *P*–1 space group. Hydrogen bonds play an important role in the 2-D planar structure of **2**. There are two types of $\mathrm{NH_4^+}$ (figure 7), one $\mathrm{NH_4^+}$ is N(4). Each N(4) connects with five oxygens, in which O(1), O(5), and O(9) are coordinated carboxyl from one $(\mathrm{NH_4})_4[\mathrm{Sm^{III}}_2(\mathrm{dtpa})_2]\cdot 10\mathrm{H_2O}$ molecule and O(4) is uncoordinated carboxyl O atoms from the other $(\mathrm{NH_4})_4[\mathrm{Sm^{III}}_2(\mathrm{dtpa})_2]\cdot 10\mathrm{H_2O}$ molecule and O(11) from lattice water. The hydrogen bond distances of N(4)…O(1), N(4)…

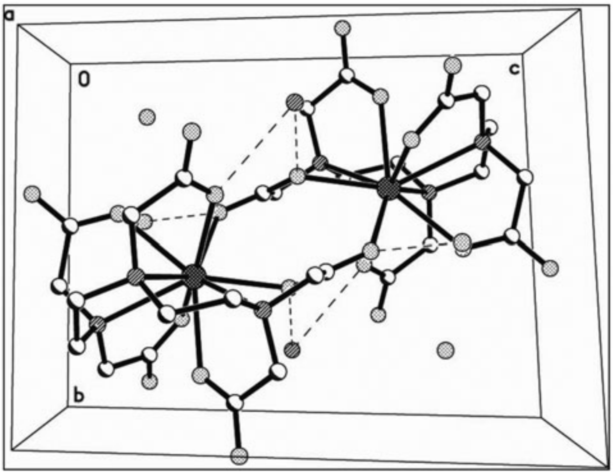

Figure 6. Arrangement of **2** in unit cell (dashed lines represent intermolecular hydrogen bonds).

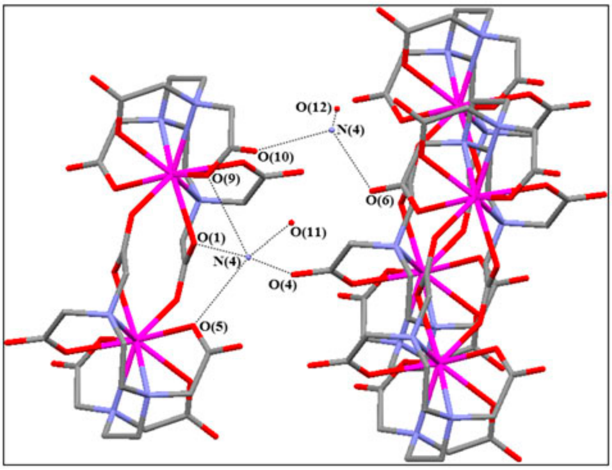

Figure 7. Bindings between NH_4^+ and $[Sm^{III}_2(dtpa)_2]^{4-}$ in **2** (dashed lines represent intermolecular hydrogen bonds).

O(4), N(4)…O(5), N(4)…O(9), and N(4)…O(11) are 2.854, 2.796, 2.941, 3.043, and 2.960 Å, respectively. The second NH_4^+ is N(5), which links two uncoordinated carboxyl O(6) and O(10) from two different $(NH_4)_4[Sm^{III}_2(dtpa)_2]\cdot 10H_2O$ molecules and O(12) from one lattice water. N(5)…O(6), N(5)…O(10), and N(5)…O(12) hydrogen bond distances are 2.894, 2.762, and 2.849 Å, respectively.

As shown in figure 8, $[Sm^{III}_2(dtpa)_2]^{4-}$ are interconnected by sharing NH_4^+ and lattice water, forming an infinite 1-D chain along the *a*-axis. The hydrogen bond distances of O(2) …O(12), O(7)…O(12), N(5)…O(12), and N(5)…O(6) are 3.038 Å, 2.983 Å, 2.849 Å, and

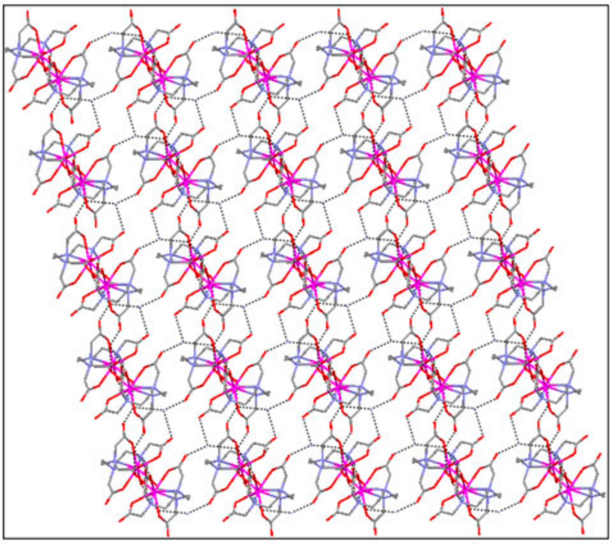

Figure 8. Polyhedral view of the 2-D ladder-like layered network of **2**.

2.895 Å, respectively. Along the *b*-axis, two neighboring $[Sm^{III}_2(dtpa)_2]^{4-}$ complex anions are connected by sharing the NH_4^+ and lattice water, with O(2)…O(12), O(4)…O(12), O(7)…O(12), N(5)…O(12), and N(5)…O(10) hydrogen bond distances of 3.038, 2.834, 2.983, 2.849, and 2.762 Å, respectively, resulting in the formation of an infinite 1-D chain. The two 1-D chains are linked by sharing the NH_4^+ and lattice water along the *ab* plane, leading to the formation of a close-knit 2-D ladder-like network structure.

4. Conclusions

Two Sm^{III} complexes with aminopolycarboxylic acid ligands (H_6ttha = triethylenetetramine-*N,N,N′,N″,N‴,N‴*-hexaacetic acid and H_5dtpa = diethylenetriamine-*N,N,N′,N″,N″*-pentaacetic acid), $(NH_4)_4[Sm^{III}_2(Httha)_2]\cdot16H_2O$ and $(NH_4)_4[Sm^{III}_2(dtpa)_2]\cdot10H_2O$, were synthesized and characterized by FT-IR spectra, thermal analyses, and single-crystal X-ray diffraction. Both adopt nine-coordinate tricapped trigonal prismatic conformation. However, due to different ligands, **1** and **2** have different crystal structures, space groups, etc. **1** adopts a binuclear nine-coordinate TC-TP conformation, different from previously reported $(enH_2)_{1.5}[Sm^{III}(ttha)]\cdot4.5H_2O$, $K_4[Eu^{III}_2(Httha)_2]\cdot13.5H_2O$, and $K_4[Sm^{III}_2(Httha)_2]\cdot14H_2O$, whose coordinate geometry around Sm^{III} or Eu^{III} are pseudo-MC-SAP. Use of ammonium as the counter ion results in two protonated amine nitrogens forming $\equiv NH^+$, causing N(4) and N(8) to not coordinate with Sm^{III}. It is different from methylamine and ethylenediamine salts of rare-earth metal complexes with ttha. As expected, **2** also takes binuclear nine-coordinate tricapped trigonal prismatic polyhedron, different from the K and Na salts of rare-earth metal complexes with dtpa, $K_2[Dy^{III}(dtpa)(H_2O)]\cdot6H_2O$ and $Na_4[Dy^{III}(dtpa)(H_2O)]_2\cdot16H_2O$, with a mononuclear nine-coordinate structure. Ammonium as the counter ion results in the formation of hydrogen bonds among complex anions, lattice water, and protonated ammonium (NH_4^+), leading to the formation of close-knit 2-D ladder-like network. Diversity of aminopolycarboxylic acid ligands and counter ion results in different molecular structures of the two Sm^{III} complexes. Therefore, we conclude that ligand structures and counter ions play a crucial role on the molecular and crystal structures of rare-earth metal complexes with aminopolycarboxylic acid ligands.

Supplementary material

CCDC 947291 $(NH_4)_4[Sm^{III}_2(Httha)_2]\cdot16H_2O$ and CCDC 959909 $(NH_4)_4[Sm^{III}_2(dtpa)_2]\cdot10H_2O$ contain the supplementary crystallographic data for this article. These data can be obtained free of charge via www.ccdc.cam.ac.uk/data_request/cif, by e-mailing data_request@ccdc.cam.ac.uk, or by contacting The Cambridge Crystallographic Data Center, 12 Union Road, Cambridge CB2 1EZ, UK; Fax: +44(0)1223 336 033.

Acknowledgments

The authors also thank our colleagues and other students for their participation in this work. Especially, we thank Professor K. Miyoshi and T. Mizuta (Faculty of Science, Hiroshima University, Japan) for instruction.

Funding

The authors greatly acknowledge the National Natural Science Foundation of China (21371084), Liaoning Provincial Department of Education Innovation Team Projects (LT2012001), Shenyang Science and Technology Plan Projects (F12-277-1-15), Liaoning University “211” Engineering Construction Project and Science Foundation of Liaoning Provincial Education Department (L2011007) for financial support.

References

[1] S.C. Manna, E. Zangrando, J. Ribas, N.R. Chaudhuri. *Polyhedron*, **25**, 1779 (2006).
[2] Y.J. Zhu, J.X. Chen, W.H. Zhang, Zh.G. Ren, Y. Zhang, J.P. Lang, S.W. Ng. *J. Organomet. Chem.*, **690**, 3479 (2005).
[3] R.M. Sink, D.C. Buster, A.D. Sherry. *Inorg. Chem.*, **29**, 3645 (1990).
[4] K. Takahashi, H. Nakamura, S. Furumoto, K. Yamamoto, H. Fukuda, A. Matsumura, Y. Yamamoto. *Bioorg. Med. Chem.*, **13**, 735 (2005).
[5] S. Laurent, L. Vander Elst, M. Wautier, C. Galaup, R.N. Muller, C. Picard. *Bioorg. Med. Chem. Lett.*, **17**, 6230 (2007).
[6] L. Li, J.H. Yang, X. Wu, Ch.X. Sun, Y. Liu, Sh.F. Liu, B.Y. Su. *Talanta*, **65**, 201 (2005).
[7] G.L. Law, K.L. Wong, C.W.Y. Man, W.T. Wong, S.W. Tsao, M.H.W. Lam, P.K.S. Lam. *J. Am. Chem. Soc.*, **130**, 3714 (2008).
[8] K.L. Wong, G.L. Law, M.B. Murphy, P.A. Tanner, W.T. Wong, P.K.S. Lam, M.H.W. Lam. *Inorg. Chem.*, **47**, 5190 (2008).
[9] S.L. Zheng, M.L. Tong, X.M. Chen. *Coord. Chem. Rev.*, **246**, 185 (2003).
[10] F.R. Richardson. *Chem. Rev.*, **82**, 541 (1982).
[11] J.G. Kang, J.P. Hong, S.K. Yoon. *J. Alloys Compd.*, **339**, 248 (2002).
[12] Z.R. Hong, W.L. Li, D.X. Zhao, C.J. Liang, X.Y. Liu, J.B. Peng, D. Zhao. *Synth. Met.*, **104**, 165 (1999).
[13] G. Prabhakar, S.H. Joshi, D.K. Ranganatha, S. Umamaheswari, M. Ananthakrishnan, N. Ramamoorthy. *Nucl. Med. Biol.*, **27**, 353 (2000).
[14] A.H. Peruski, L.F. Peruski Jr. *Clin. Diagn. Lab. Immun.*, **10**, 506 (2003).
[15] Y. Menda, D.L. Bushnell, R.D. Williams, S. Miller, M.O. Thomas. *Clin. Nucl. Med.*, **25**, 698 (2000).
[16] N. Pandit-Taskar, M. Batraki, C.R. Divgi. *J. Nucl. Med.*, **45**, 1358 (2004).
[17] W. Fan, L.X. Chen, X.W. Liu, Q. Tang, S.F. Zhi, Z.Y. Zeng. *Chinese-German J. Clin. Oncol.*, **6**, 396 (2007).
[18] V. Hušák, M. Mysliveček. *J. Radioanal. Nucl. Chem. Art.*, **209**, 361 (1996).
[19] W.A. Volkert, T.J. Hoffman. *Chem. Rev.*, **99**, 2269 (1999).
[20] Y. Menda, D.L. Bushnell, R.D. Williams, S. Miller, M.R. Thomas. *Clin. Nucl. Med.*, **25**, 698 (2000).
[21] S. Jurisson, D. Berning, W. Jia, D. Ma. *Chem. Rev.*, **93**, 1137 (1993).
[22] M. Neves, L. Gano, N. Pereira, M.C. Costa, M.R. Costa, M. Chandia, M. Rosado, R. Fausto. *Nucl. Med. Biol.*, **29**, 329 (2002).
[23] J. Wang, P. Hu, B. Liu, X. Chen, L.Q. Zhang, G.X. Han, R. Xu, X.D. Zhang. *Russ. J. Inorg. Chem.*, **55**, 1567 (2010).
[24] J.Q. Gao, D. Li, J. Wang, X.D. Jin, T. Wu, K. Li, P.L. Kang, X.D. Zhang. *J. Coord. Chem.*, **64**, 2234 (2011).
[25] J. Wang, X.Zh. Liu, Zh.H. Zhang, X.D. Zhang, G.R. Gao, Y.M. Kong, Y. Li. *Russ. J. Coord. Chem.*, **32**, 590 (2006).
[26] J. Wang, Y. Wang, Zh.H. Zhang, X.D. Zhang, X.Y. Liu, X.Zh. Liu, Zh.R. Liu, Y. Zhang, J. Tong, P. Zhang. *J. Coord. Chem.*, **59**, 295 (2006).
[27] J. Wang, X.Z. Liu, Z.H. Zhang, X.D. Zhang, G.R. Gao, Y.M. Kong, Y. Li. *J. Coord. Chem.*, **59**, 2103 (2006).
[28] J. Wang, X.Zh. Liu, X.F. Wang, G.R. Gao, Zh.Q. Xing, X.D. Zhang, R. Xu. *J. Struct. Chem.*, **49**, 75 (2008).
[29] Y. Inomata, T. Sunakawa, F.S. Howell. *J. Mol. Struct.*, **648**, 81 (2003).
[30] J. Wang, Y. Wang, X.-D. Zhang, Z.-H. Zhang, Y. Zhang, L.P. Kang, H. Li. *J. Coord. Chem.*, **58**, 921 (2005).
[31] J. Wang, G.R. Gao, Zh.H. Zhang, X.D. Zhang, Y.J. Wang. *J. Coord. Chem.*, **60**, 2221 (2007).